

Fig. 5. Composite spectra extracted from large areas with the best-fit 1-temperature Raymond-Smith model (solid lines). (a) "field 1 north" including NGC 1977, (b) "Field 1 south," (c) "Field 2 north" including OMC-2, (d) "Field 2 south" including Orion Trapezium, (e) "Trapezium region" extracted from a 6' diameter region centered on the Trapezium, and (f) "outer Trapezium region." Data from SIS 0 and SIS 1 were combined, as were GIS 2 and GIS 3.

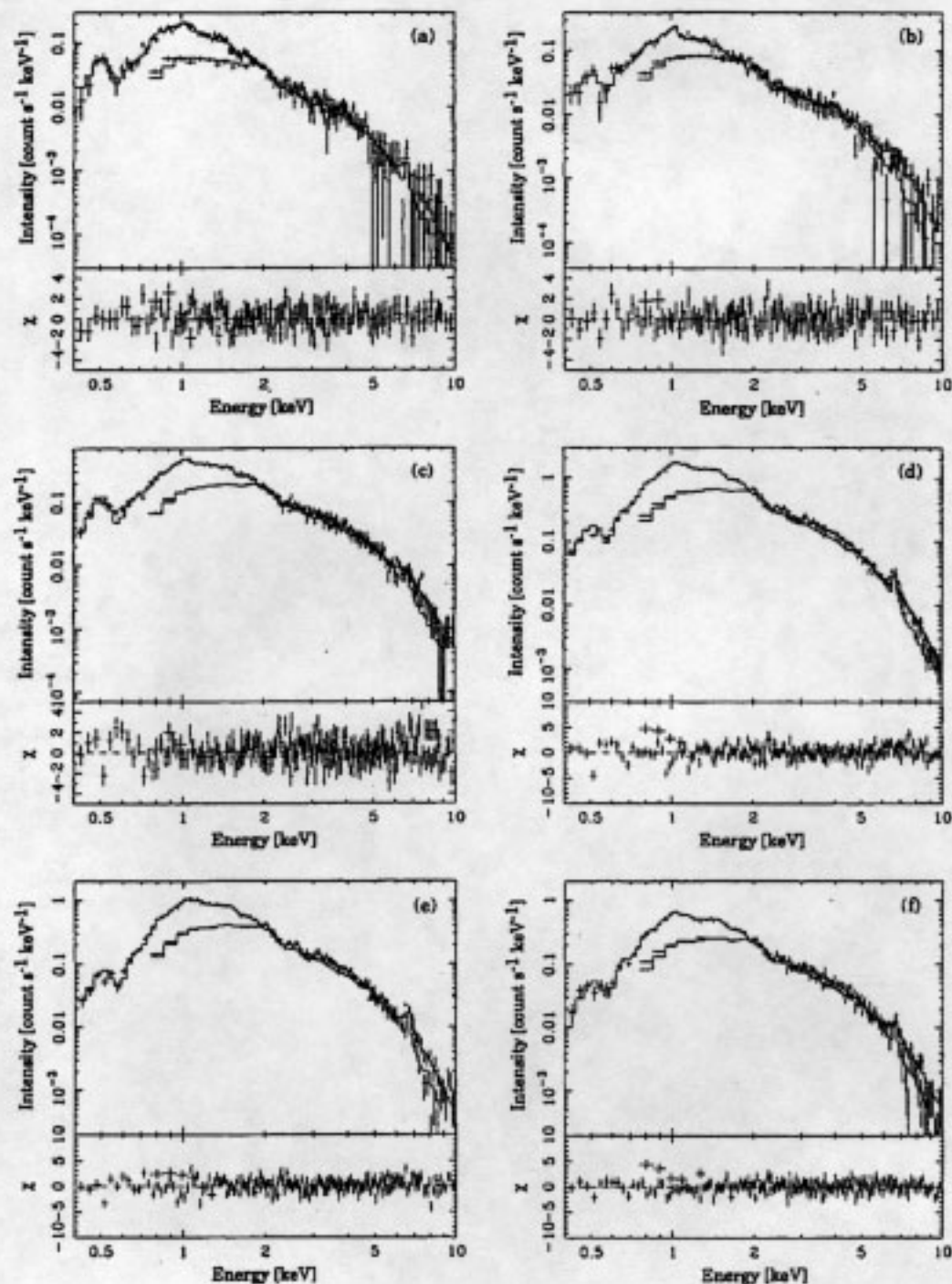


Fig. 6. Same as figure 4, but with the 2-temperature Raymond-Smith model.

seen in all regions containing luminous IR sources, it is most obvious in the Mon R2 region.

3.4.4. Orion Nebula (M42) and NGC 1977

The H II region M42, the most luminous region in our study, is located in the midsection of a 1° long north-south filament of high density [on average, $n(H_2) > 10^4 \text{ cm}^{-3}$] gas in the northern portion of the Orion A molecular cloud (see the photographic illustration of the ^{12}CO emission in Bally et al. 1987a). The H II region forms a blister on the near side of the molecular ridge which contains a high-luminosity embedded source, IRc 2, located at a projected distance of only $1'$ north of the Trapezium cluster (which is responsible for ionizing the visible nebula). The infrared morphology of M42 is very different from that of the molecular cloud; all four IRAS bands show M42 to consist of a very bright core surrounded by a ring of emission located just outside the optical boundary of the H II region.

A less luminous and more evolved H II region, NGC 1977, is located at the northern end of the molecular ridge. Just like M42, this region is also surrounded by a ring of infrared emission, a morphology very different from that of the associated molecular cloud.

In a $15' \times 12'$ region which contains the core of the Orion A cloud and the Orion Nebula (M42), neither the $100\mu\text{m}$ intensity nor opacity appears to correlate well with $I(^{12}\text{CO})$ (Fig. 8). However, these quantities do correlate with $I(^{12}\text{CO})$ up to about 200 K km s^{-1} corresponding to $I(100\mu\text{m})$ of about 20 GJy sr^{-1} . At higher values of $I(^{12}\text{CO})$, the dust opacity and $100\mu\text{m}$ intensity do not vary. These high values correspond to the BN-KL source and the high-velocity outflow surrounding IRc 2. The north-south cuts through the BN-KL source in all four bands show that the peaks in 100 and $60\mu\text{m}$ emission are flat, while 25 and $12\mu\text{m}$ emission exhibit sharp peaks, suggesting saturation in the long-wavelength bands.

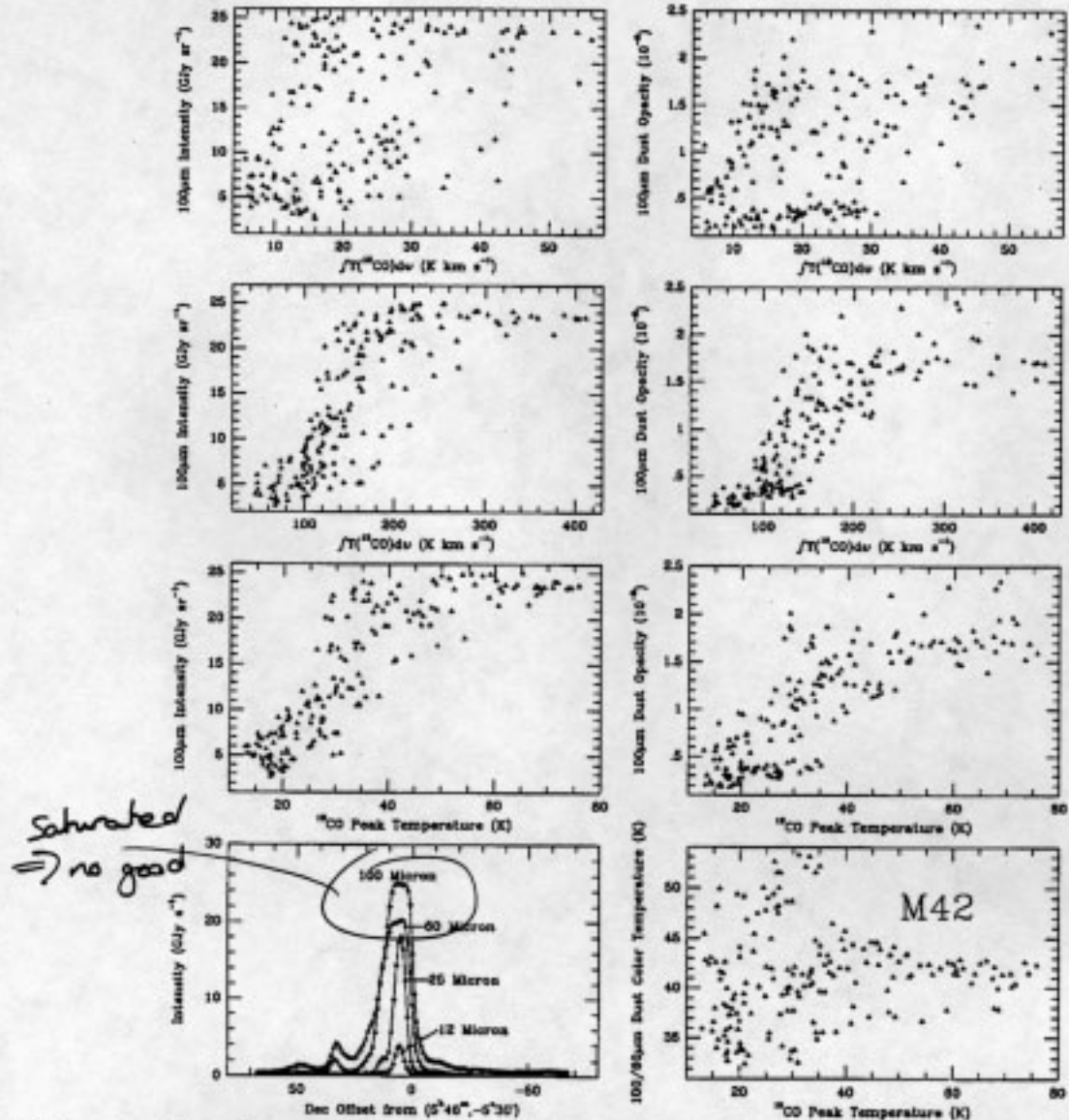


FIG. 8.—Comparison of dust and gas properties near the Orion Nebula (M42 region). Slices of intensities in all the four bands from north to south across the infrared peak of the H II region are also shown.

1975 AP + SS λ *Conditio* vol 36: 409

ORION A

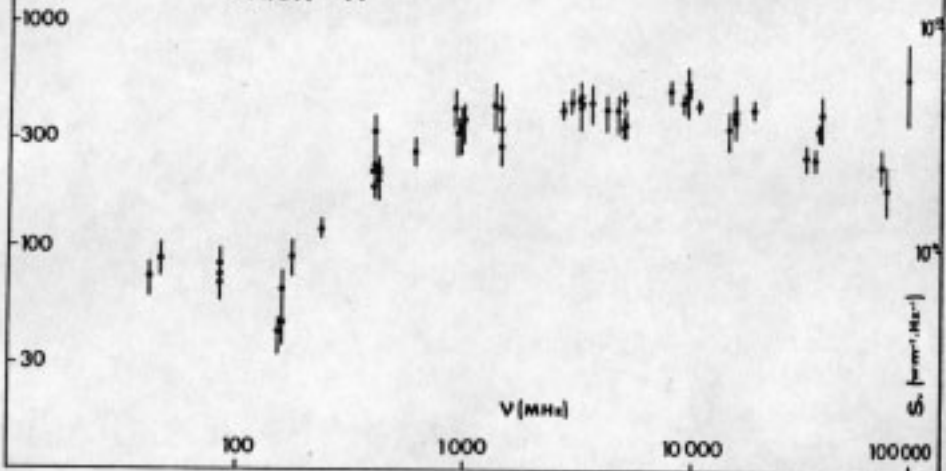


Fig. 1. The radio spectrum of the Orion nebula (M42 and M43).

TABLE I
Orion nebula - Radio spectrum

1 No.	2 Frequency ν (MHz)	3 Wavelength λ (m, cm or mm)	4 Flux density S_f (fu) ($1 \text{ fu} = 10^{-26}$ $\text{W m}^{-2} \text{ Hz}^{-1}$)	5 References
1	42.2	7.10 m	73.7 ± 15	Haynes and Hamilton (1968)
2	47.3	6.35 m	89.0 ± 18	Haynes and Hamilton (1968)
3	85.5	3.55 m	69 ± 14	Mills <i>et al.</i> (1956)
4	86.0	3.50 m	85.0 ± 17	Risbeth (1958)
5	86.0	3.50 m	74 ± 15	Mills <i>et al.</i> (1956)
6	153	1.96 m	41.6 ± 9	Hamilton and Haynes (1967)
7	159	1.90 m	65 ± 13	Risbeth (1958)
8	159	1.90 m	45 ± 9	Edge <i>et al.</i> (1959)
9	178	1.80 m	90 ± 18	Conway <i>et al.</i> (1963)
10	240	1.25 m	120 ± 12	Menon and Terzian (p.c.) (1964)
11	400	75 cm	230 ± 46	Seeger <i>et al.</i> (1956)
12	400	75 cm	325 ± 65	Seeger <i>et al.</i> (1961)
13	400	75 cm	220 ± 44	Howard <i>et al.</i> (1965)
14	405	74 cm	188 ± 9	Menon and Terzian (p.c.) (1965)
15	408	73.5 cm	200 ± 40	Long <i>et al.</i> (1963)

1 No.	2 Frequency ν (MHz)	3 Wavelength λ (m, cm or mm)	4 Flux density S_f (fu) ($1 \text{ fu} = 10^{-26}$ $\text{W m}^{-2} \text{ Hz}^{-1}$)	5 References
16	408	73.5 cm	213 ± 17	Mills and Shaver (1968)
17	408	73.5 cm	213 ± 43	Parkes Catalogue*
18	600	50 cm	268 ± 40	Piddington and Trent (1956)
19	910	33 cm	420 ± 84	Denisse <i>et al.</i> (1957)
20	960	31 cm	342 ± 10	Harris and Roberts (1960)
21	960	31 cm	360 ± 72	Wilson and Bolton (1960)
22	960	31 cm	343 ± 68	Conway <i>et al.</i> (1963)
23	1370	22 cm	430 ± 86	Westerhout (1958)
24	1410	21.3 cm	289 ± 58	Parkes Catalogue*
25	1420	21 cm	420 ± 84	Hagen <i>et al.</i> (1954)
26	1420	21 cm	331 ± 50	Hagen <i>et al.</i> (1954)
27	2700	11 cm	411 ± 41	Altenhoff <i>et al.</i> (1961)
28	2930	10.3 cm	454 ± 55	Sloaneker and Nichols (1960)
29	3130	9.6 cm	412 ± 62	Kuzmin <i>et al.</i> (1960)
30	3200	9.4 cm	426 ± 43	Haddock <i>et al.</i> (1954)
31	3200	9.4 cm	450 ± 90	Pariskii (1961)
32	3200	9.4 cm	460 ± 12	Medd (p.c.) (1964)
33	3600	8.3 cm	450 ± 90	Pariskii (1961)
34	4170	7.2 cm	410 ± 82	Yokoi <i>et al.</i> (1966)
35	4700	6.4 cm	410 ± 82	Golnev <i>et al.</i> (1965)
36	5000	6 cm	342 ± 23	Mezger and Henderson (1967)
37	5000	6 cm	470 ± 33	Baars <i>et al.</i> (1965)
38	5000	6 cm	344 ± 69	Gardner and Morimoto (1968)
39	8000	3.7 cm	502 ± 60	Menon (1961)
40	9360	3.2 cm	450 ± 30	Lazarevskii <i>et al.</i> (1963)
41	9400	3.2 cm	540 ± 108	Kaidanovskii <i>et al.</i> (1955)
42	9400	3.2 cm	480 ± 96	Zakharenkov <i>et al.</i> (1963)
43	9520	3.15 cm	480 ± 96	Haddock and McCullough (1955)
44	10700	2.8 cm	434 ± 20	McLeod and Doherty (1968)
45	14500	2 cm	343 ± 69	Baars <i>et al.</i> (1965)
46	15350	1.95 cm	390 ± 79	Terzian <i>et al.</i> (1968)
47	15350	1.95 cm	400 ± 80	Schraml and Mezger (1969)
48	15550	1.94 cm	365 ± 21	Gordon (1969)
49	18750	1.6 cm	420 ± 42	Kuzmin and Salomonovich (1963)
50	31400	9.55 mm	253 ± 37	Johnston and Hobbs (1969)
51	35000	8.5 mm	250 ± 30	Tolbert (1965)
52	36500	8.2 mm	330 ± 30	Sorochenko and Berulis (1970)
53	37000	8.1 mm	500 ± 100	Kuzmin and Salomonovich (1963)
54	67800	4.3 mm	233 ± 40	Hobbs <i>et al.</i> (1969)
55	72800	4.1 mm	182 ± 45	Kaifu <i>et al.</i> (1973)
56	94000	3.2 mm	585 ± 200	Tolbert (1965)

* Parkes Catalogue = Bolton *et al.* (1964); Price and Milne (1965); Day *et al.* (1966).
(p.c.) = private communication cited in Baars *et al.* (1965).

DECLINATION (1950.0)

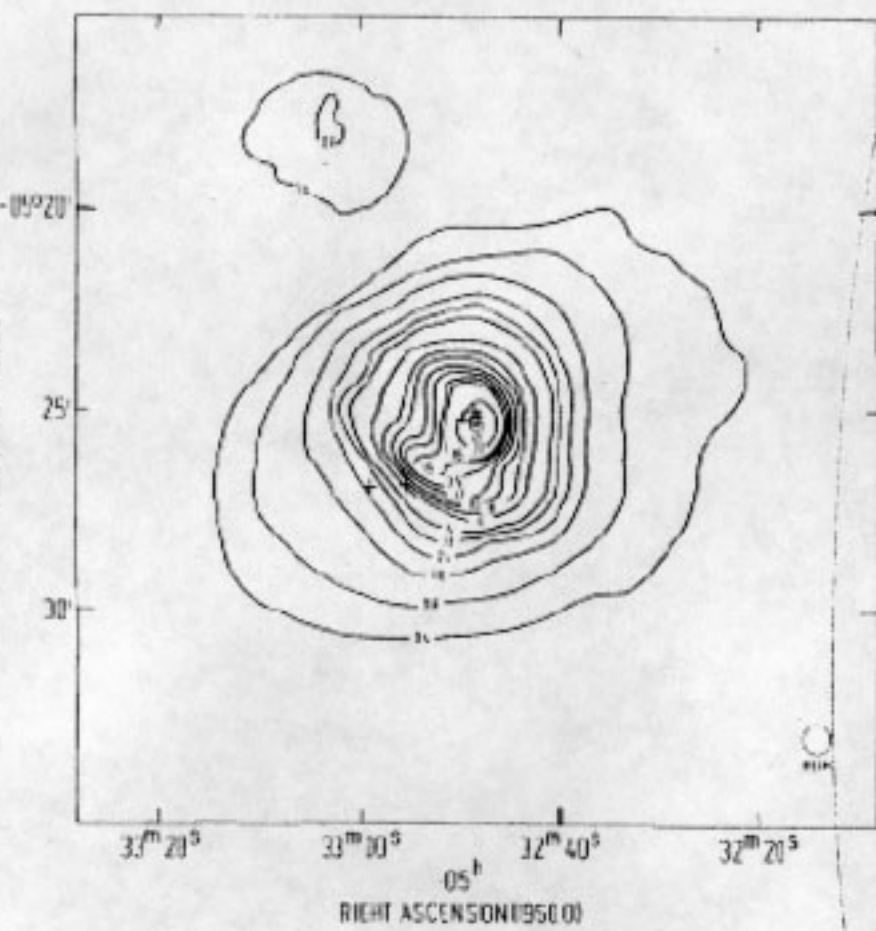


Fig. 2. The radio continuum map, as in Fig. 1, with crosses showing the positions of the 4 Trapezium stars and the two θ Orionis stars.

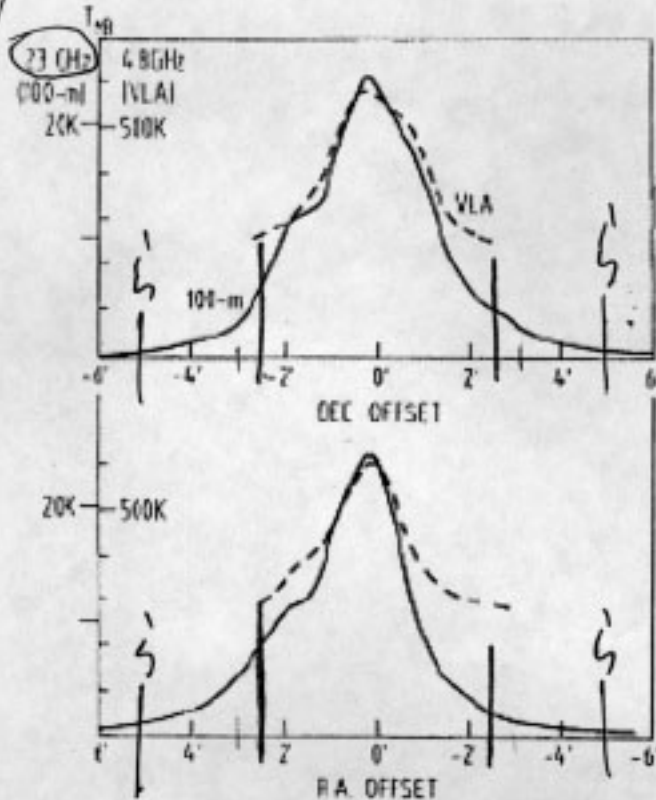


Fig. 3. Cuts in RA and Dec through the peak of the continuum ($RA = 05^{\circ}32'48''$, $Dec = -05^{\circ}25'30''$ (1950.0)) are shown as solid lines. The dashed curves are taken from the VLA map of Johnston et al. (1983), made at 4.8 GHz and smoothed to an angular resolution of $28''$. The main beam brightness temperature scale, T_B , on the far left (marked 23 GHz) refers to our 100-m data. To the right, marked 4.8 GHz, is the VLA temperature scale in T_B . The temperatures are arranged to agree if the continuum were an optically thin plasma.

TABLE 3
TOTAL NEBULAR FLUXES AND RELATIVE SURFACE BRIGHTNESS RATIOS

Bin	Limiting Values of H(1820 Å)	F_{1400}^*	F_{1820}^*	F_{2240}^*	F_{2620}^*	$(S/F_*)_{1400}$	$(S/F_*)_{2240}$	$(S/F_*)_{2620}$	$\langle r \rangle$ (arcmin)
1	≤ 8	2.48 ^b	1.40 ^b	0.927 ^b	0.910	1.06 ^b	1.41 ^b	1.75 ^b	22.7
2	9-16	1.32	0.744	0.414	0.485	1.06	1.41	1.75	17.6
3	17-32	1.61	0.933	0.590	0.532	1.03	1.34	1.53	13.6
4	33-64	2.39	1.37	0.812	0.742	1.04	1.26	1.46	10.4
5	65-128	2.51	1.32	0.791	0.704	1.14	1.38	1.44	7.5
6	129-256	3.22	1.61	0.972	0.773	1.19	1.28	1.29	6.0
7	257-512	6.47	3.04	1.69	1.34	1.27	1.18	1.19	4.4
8	513-1024	4.94	2.42	1.24	0.945	1.22	1.09	1.05	2.6
9	1025-2048	5.19	2.33	1.21	1.04	1.33	1.10	1.20	2.0
10	2049-4096	4.69	1.98	0.987	0.781	1.42	1.06	1.06	1.8
11	> 4096	2.82 ^c	1.19 ^c	0.592 ^c	0.469 ^c
Total		37.6	18.3	10.3	8.72	1.23	1.20	1.28	
Trapezium		13.9	8.31	3.91	3.09				
Total/Trapezium		2.7	2.2	2.6	2.8				
$\theta^1 + \theta^2$ On		27.9	16.1	8.06	6.22				
Total/ $\theta^1 + \theta^2$		1.35	1.14	1.28	1.40				

^a In 10^{-10} ergs cm^{-2} s^{-1} \AA^{-1} .^b For bin 1 ($H_{1820} < 8$), F_{1400} , F_{1820} , and F_{2240} were determined by requiring that their ratios to F_{2620} be the same as for bin 2.^c For bin 11 ($H_{1820} > 4096$), F_{1400} , F_{1820} , F_{2240} , and F_{2620} were determined by requiring that the mean surface brightness be the same as for bin 10.

Spectrum Of The Orion Nebula. (Central 5 ArcMinutes)

Curves fit by eye.

- Data points are ones taken from the literature as described in the notes accompanying these graphs.

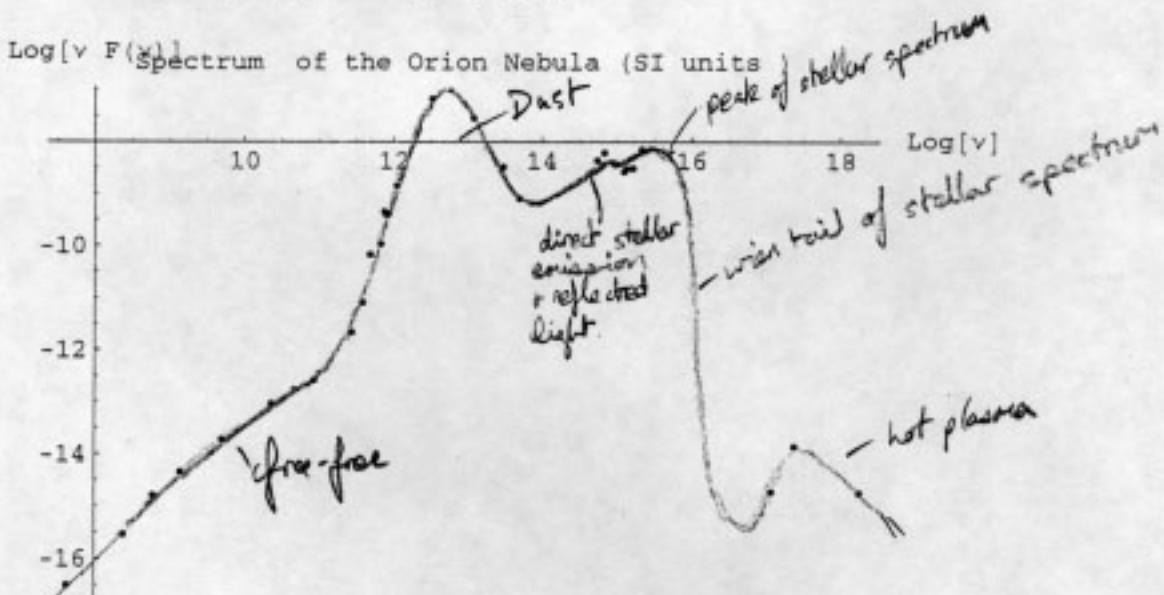
```
In[75]:= linear = {{42^6, 74}, {240^6, 120}, {600^6, 268},  
{1.4^9, 324}, {5^9, 380}, {23^9, 400}, {86^9, 307}, {273^9, 800},  
{380^9, 2136}, {480^9, 14000}, {670^9, 16000}, {750^9, 60000},  
{790^9, 50000}, {850^9, 48000}, {1.1^12, 0.13^6}, {3.3^12, 2^6},  
{1.2^13, 0.24^6}, {3^13, 11000}, {5^13, 1620}, {5.45^14, 810},  
{6.8^14, 910}, {1.24^15, 215}, {1.33^15, 230}, {1.64^15, 190},  
{2.14^15, 333}, {1.2^17, 1.6^-6}, {2.41^17, 5.8^-6}, {1.8^18, 1^-7}};
```

```
In[76]:= nufnulin = linear;
```

```
In[77]:= Do[nufnulin[[i, 2]] = linear[[i, 2]]*linear[[i, 1]]*1^(-26), {i, 1, 28}]
```

```
In[78]:= nufnulog = N[Log[10, nufnulin]];
```

```
In[85]:= ListPlot[nufnulog, PlotJoined -> False,  
PlotLabel -> "Spectrum of the Orion Nebula (SI units )",  
AxesLabel -> {"Log[v]", "Log[v F(v)]"}]
```



```
Out[85]= - Graphics -
```

the units used are : $F[\text{W m}^{-2}\text{Hz}^{-1}]$
 $v[\text{Hz}]$

The straight lines are of course artifacts of the poor resolution I have in some parts of the spectrum.

```
In[80]:= fnulin = linear;
```

```
In[81]:= Do[fnulin[[i, 2]] = linear[[i, 2]]*1^(-26), {i, 1, 28}]
```

```
In[82]:= fnulog = N[Log[10, fnulin]];
```